Supporting Information for

Morphology-Controlled Synthesis of CoMoO4 Nanoarchitectures Anchored on Carbon Cloth for High-Efficiency Oxygen Oxidation Reaction

Feifei Wang,[a, ‡] Juan Zhao,[a, ‡] Wen Tian,[a] Zhufeng Hu,[a] Xingbin Lv,[a] Hualian Zhang,[a] Hairong Yue,[a] Yuxin Zhang,[c] Junyi Ji,[a, b,]* Wei Jiang[a]

[a] *School of Chemical Engineering, Sichuan University, Chengdu 610065, P. R. China*

[b] *State Key Laboratory of Polymer Materials Engineering, Sichuan University, Chengdu 610065, P. R. China*

[c] *College of Material Science and Engineering, Chongqing University, Chongqing, 400044, P. R. China*

** Corresponding author. E-mail addresses:*
Junyi Ji, E-mail: junyiji@scu.edu.cn

‡ The authors contribute equal to this manuscript.

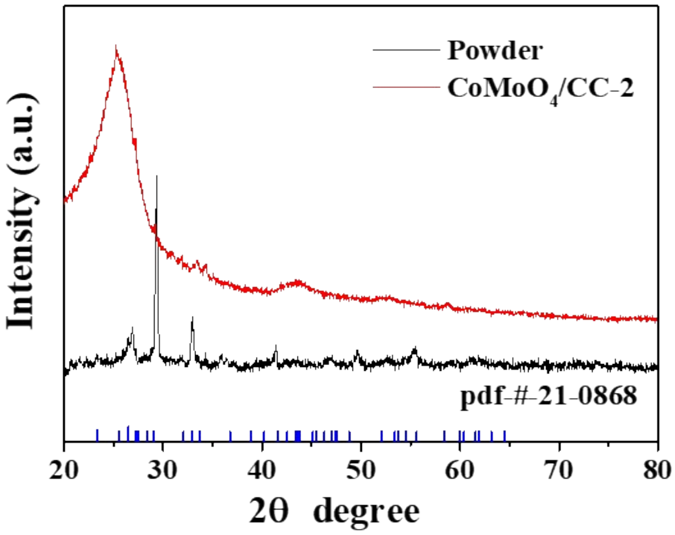

Figure S1 XRD patterns of theCoMoO$_4$/CC-2 and the corresponding powder collected during the hydrothermal process.

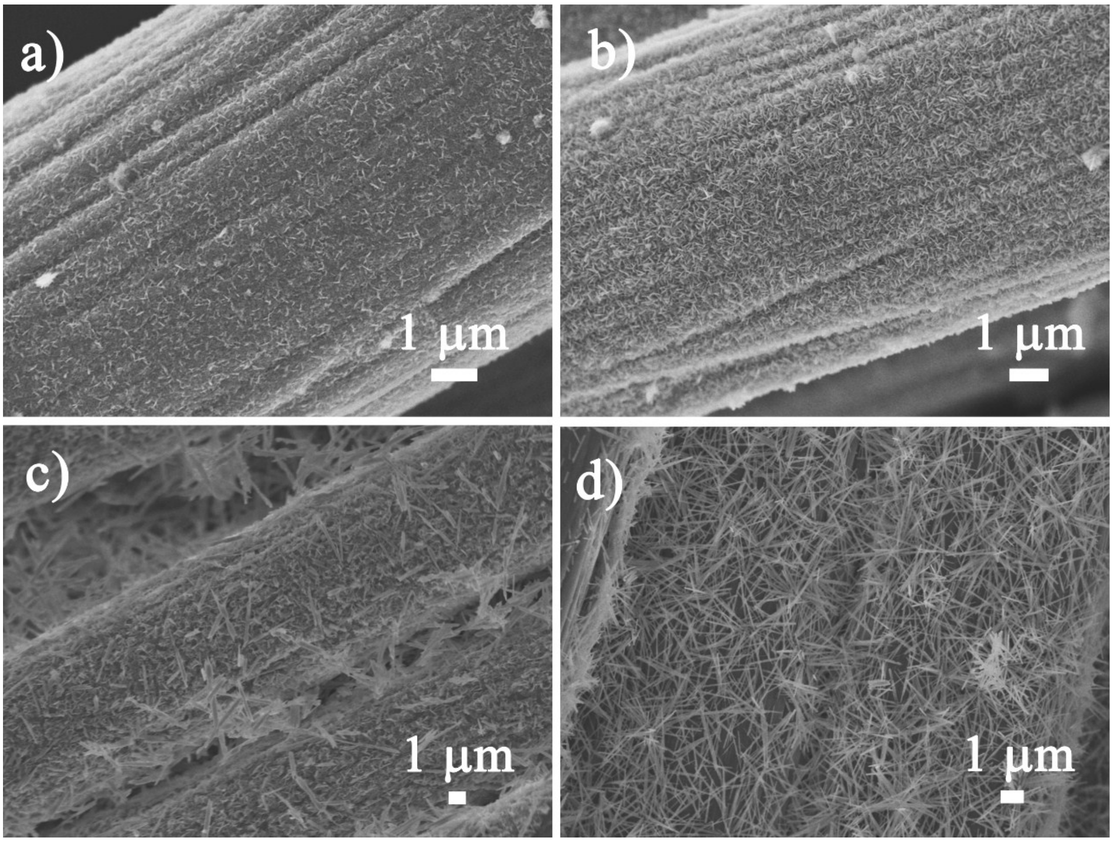

Figure S2 Low magnification SEM images of the a) $CoMoO_4$/CC-1, b) $CoMoO_4$/CC-2 and c) $CoMoO_4$/CC-3 and d) $CoMoO_4$/CC-4.

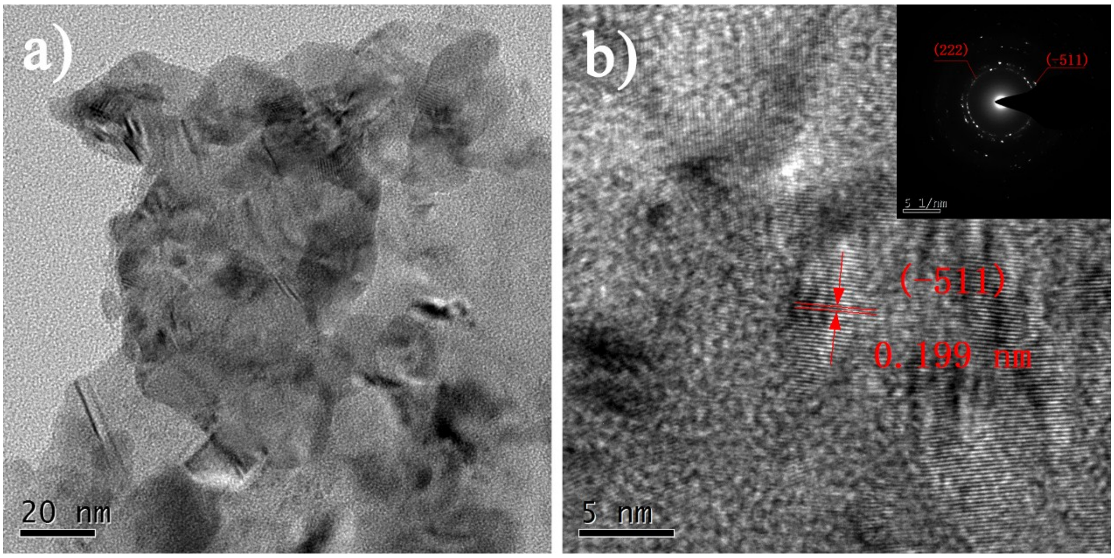

Figure S3 TEM images of the $CoMoO_4$/CC-3 composite, a) low magnification images, b) high magnification images and the SAED pattern.

Figure S3a shows that the nanosheets and nanorods are coexisted in the $CoMoO_4$/CC-3 composite. As shown in figure S3b, the lattice fringe of 0.199 nm can be ascribed to the (-511) plane of $CoMoO_4$. Moreover, the inset in figure S3b also reveals the polycrystalline structure of the $CoMoO_4$/CC-3 composite.

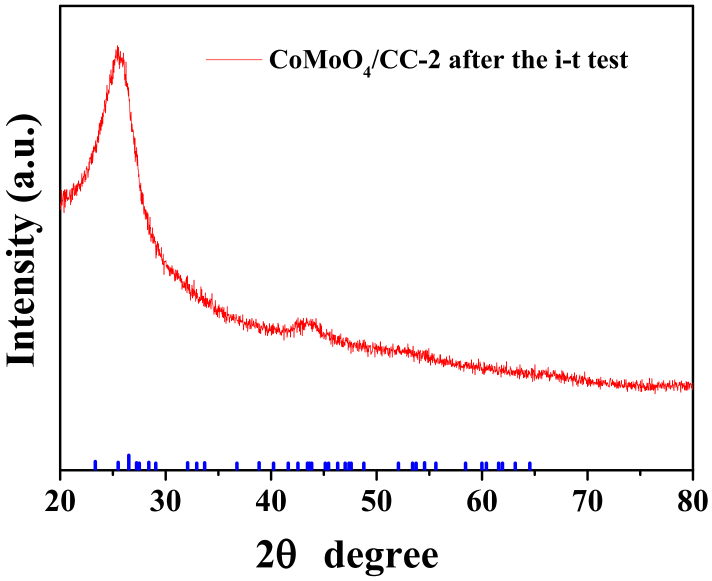

Figure S4 XRD patterns of the $CoMoO_4$/CC-2 composite after the i-t test.

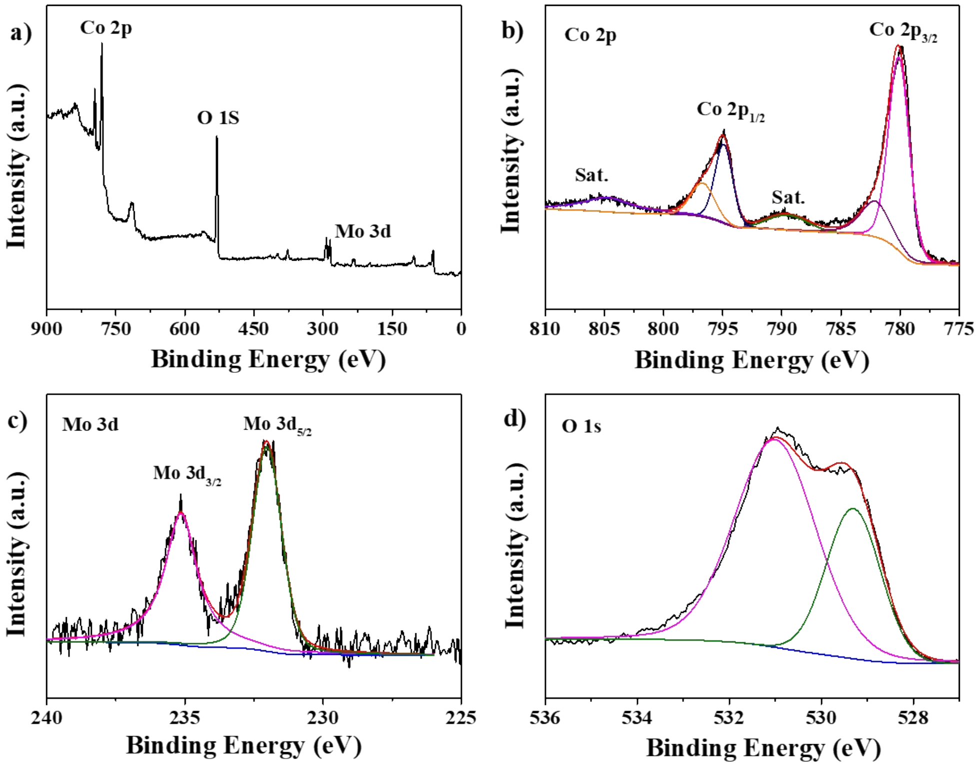

Figure S5 XPS spectra of a) full survey, b) Co 2p, c) Mo 2d and d) O 1s of the $CoMoO_4$/CC-2 electrode after the i-t test.

Figure S5 shows the XPS results of the $CoMoO_4$/CC-2 composite after the i-t test. The full survey spectrum in **figure S5a** exhibits the coexistence of the Mo, Co and O elements in the composite. As depicted in **figure S5b**, the peaks located at 780.1 eV and 795.1 eV are in line with Co^{3+} species, demonstrating part of the Co (Ⅱ) was further oxidized into Co (Ⅲ) during the stability test. Moreover, the peaks of Mo element remained almost unchanged according to **figure S5c**, while the peaks of O 1s shift to the lower binding energy, which may be due to the oxidation of the Co elements.

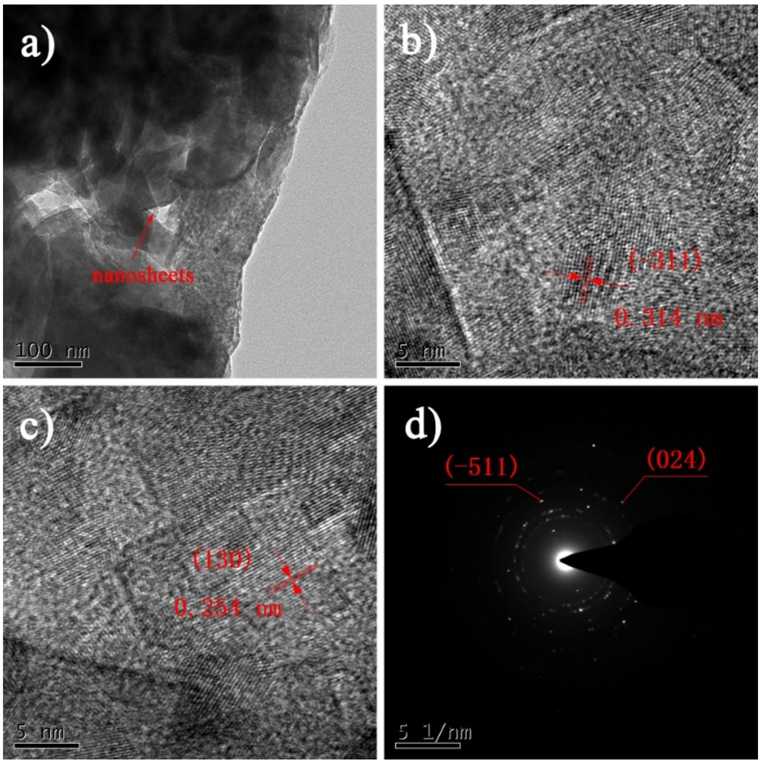

Figure S6 TEM images of the $CoMoO_4$/CC-2 composite after the long cycling test, a) the $CoMoO_4$ nanosheets, b, c) the high-resolution image of the $CoMoO_4$ nanosheets and d) the SAED pattern acquired from $CoMoO_4$ nanosheets.

Figure S6a shows the stacked $CoMoO_4$ nanosheets, demonstrating the part agglomeration of the $CoMoO_4$ composite. In figure S6b, the lattice fringe of 0.314 nm can be related to the (-311) plane of $CoMoO_4$. Moreover, it is important to note in Figure S6 that CoOOH crystal phases appear in the $CoMoO_4$ composite after the cyclic test and the lattice fringe of 0.254 nm can be ascribed to the (130) plane of CoOOH (PDF#26-0846), which illustrates the oxidation process of Co^{2+} in the stability test process. In addition, the crystalline structure is further certified by the selected area electron diffraction (SAED) pattern (**Figure S6d**), illustrating the structural stability of the $CoMoO_4$ composite.

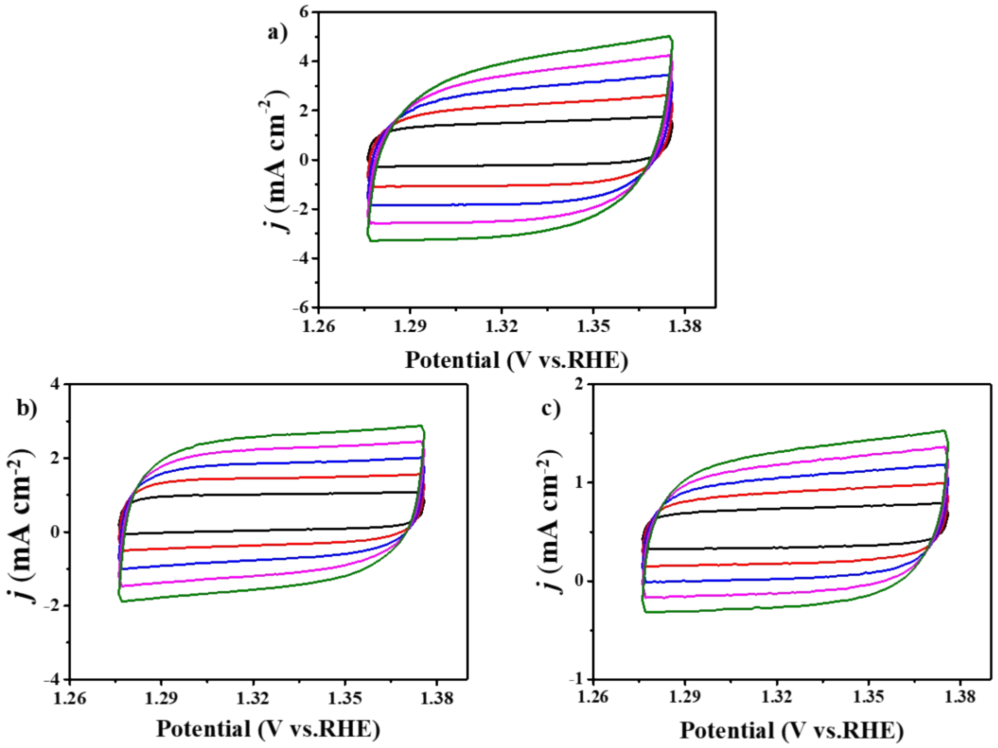

Figure S7 CV curves of a) $CoMoO_4$/CC-1, b) $CoMoO_4$/CC-3 and c) $CoMoO_4$/CC-4 at different scan rates from 10 to 50 mV s^{-1}.

Table S1 The loading mass of the as-prepared composites.

Composites	**$CoMoO_4$/CC-1**	**$CoMoO_4$/CC-2**	**$CoMoO_4$/CC-3**	**$CoMoO_4$/CC-4**
Mass (mg cm^{-2})	**0.13**	**0.75**	**0.82**	**0.19**

Table S2 The atomic ratio of Co and Mo elements of the $CoMoO_4$/CC-2 composite in the XPS results.

Elements	**Mo**	**Co**
Atomic %	**8.07%**	**17.29%**

Table S3 Comparison of the OER performance of $CoMoO_4$/CC with recently reported materials in alkaline solution.

Catalysts	Current density (mA cm^{-2})	Overpotential (mV)	Ref.
$CoMoO_4$/CC	**15**	**286**	**This work**
Co_3O_4/$CoMoO_4$	**10**	**318**	**1**
$NiCo_2O_4$@$CoMoO_4$/NF	**20**	**265**	**2**
$CoMoO_4$/CC	**10**	**290**	**3**
$CoMoO_4$	**10**	**430**	**4**
$CoMoO_4$ nanorod	**10**	**343**	**5**
$CoMoO_4$	**20**	**370**	**6**

Reference

1. L. Zhang, T. Mi, M. A. Ziaee, L. Liang and R. Wang, *J. Mater. Chem. A*, 2018, **6**, 1639-1647.
2. Y. Gong, Y. Zhi, L. Yu, J. Wang, H. Pan and Z. Xu, *J. Mater. Chem. A*, 2018, **6**, 16950-16958.
3. J. Meng, J.-Q. Fu, X. Yang, M.-J. Wei, S. Liang, H.-Y. Zang, H.-Q. Tan, Y.-H. Wang and Y.-G. Li, *Inorg. Chem. Front.*, 2017, **4**, 1791-1797.
4. M. Rodriguez, M. C. P. Stolzemburg, C. G. O. Bruziquesi, A. C. Silva, C. G. Abreu, K. P. F. Siqueira, L. C. A. Oliveira, M. S. Pires, L. C. T. Lacerda, T. C. Ramalho, A. Dias and M. C. Pereira, *Crystengcomm*, 2018, **20**, 5592-5601.
5. X. Liu, Y. Yang and S. Guan, *Chem. Phys. Lett.*, 2017, **675**, 11-14.
6. X. Yan, L. Tian, S. Atkins, Y. Liu, J. Murowchick and X. Chen, *ACS Sustainable Chem. Eng.*, 2016, **4**, 3743-3749.